Interfacial behaviour of various liquid electrode/β″–alumina systems

M. W. BREITER, B. DUNN[†]

General Electric Corporate Research and Development, PO Box 8, Schenectady, NY 12301, USA

Three different liquid electrode/sodium β''-alumina interfaces were investigated. The $NaNO_3/\beta''$-alumina interface displays ohmic behaviour although the resistance is somewhat larger than expected. The sodium/β''-alumina interface exhibits asymmetric resistance with respect to d.c. current flow. Cyclic voltammetry results suggest that a Na_2O film is being modified electrochemically during the sweeps. When a sodium amalgam electrode is utilized, the film, if it is present, has very little effect. The asymmetric resistance is not observed and there is good agreement between d.c. and a.c. resistances after only a small amount of sodium deposition.

1. Introduction

Asymmetric resistance for certain sodium β''-alumina ceramics has recently been described [1, 2]. The phenomenon was observed with respect to the direction of d.c. current flow in sodium/sodium β''-alumina/sodium nitrate cells and in sodium/sodium β''-alumina/sodium poly-sulphide cells. In both cases the asymmetric behaviour involved a larger effective resistance during discharge (anodic sodium dissolution) than during charge (cathodic sodium deposition). Experimental results were also able to establish that the asymmetry arises primarily from the sodium/β''-alumina interface. The present paper is concerned with the behaviour of different liquid electrode/sodium β''-interfaces. In addition to liquid sodium, molten sodium nitrate and various sodium amalgams have been investigated. The results indicate that in all three instances, distinctly different charge-transfer processes are involved.

2. Experimental

The solid electrolyte tube used in all of the experiments had a nominal composition of (in weight per cent) $9.6\%Na_2O + 0.75\% Li_2O$, with the balance being Al_2O_3 with a β'' content of approxi-

mately 80%. The time dependence of its asymmetric behaviour has recently been evaluated [3]. Fabrication of the tube has been described elsewhere [4].

Measurements were made at $350°C$ in the following cells:

(a) Cu/Al/Na/β''-alumina/$NaNO_3$/Pt/Cu,
(b) Cu/Al/Hg(Na)/β''-alumina/$NaNO_3$/Pt/Cu,
(c) Cu/Pt/$NaNO_3$/β''-alumina/$NaNO_3$/Pt/Cu.

The arrangement for Cells (a) and (b) was similar to that used previously [1] and is shown in Fig. 1a. A platinum probe served as the reference electrode inside the molten $NaNO_3$. This probe was sufficiently close to the outer surface of the tube that the ohmic potential drop inside the molten salt could be neglected. The counter electrode (not shown) was located in the narrower compartment of the U-shaped Vycor vessel. In Cell (c) (Fig. 1b) a platinum wire, protruding slightly from the lower end of a thin α-alumina tube, served as the inner reference electrode. The platinum counter electrode was wrapped around the outside of the α-alumina tube. This configuration was used to determine the radial resistance of β- and β''-aluminas in nonaqueous electrolytes [5].

Cyclic voltammetry was used in Cell (a) to investigate the asymmetric response of the liquid sodium/β''-alumina interface. A linear sweep was

[†] Present address: Department of Materials Science, UCLA, Los Angeles, CA 90024, USA.

(a)   (b)
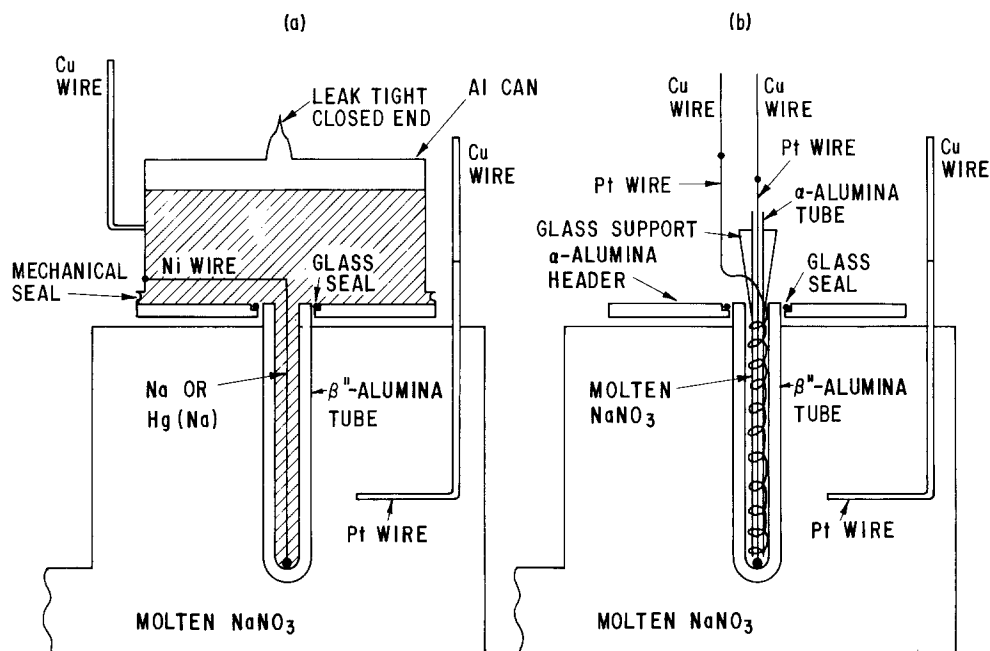

Fig. 1. (a) Schematic diagram of Cell (a) or Cell (b); (b) schematic diagram of Cell (c).

applied potentiostatically between the sodium electrode and the platinum reference electrode. Sweep rates between 10^{-2} and 10^2 V s^{-1} were used. The potential range of the scans was restricted by the maximum current output (1 A) of the potentiostat (Princeton Applied Research Model 173, with Model 175 programmer). The current–voltage curves were stored on an oscilloscope (Nicolet Model 206) and transferred on to an X–Y recorder. Critical values were obtained directly from the digital read-out of the oscilloscope.

The experiments with Cell (b) involved separate d.c. and a.c. circuits. D.c. and a.c. currents were imposed through ohmic resistors which were at least 10^3 larger than the respective cell resistances. This reduced the mutual interference of the two circuits to a negligible level. Small amplitude a.c. signals were supplied by a function generator (Hewlett-Packard Model 203A). The a.c. cell voltage was measured by a lock-in analyser (Princeton Applied Research Model 5204) with a separate channel from the function generator supplying the reference signal. Both amplitude and phase angle were read directly from the analyser. The small phase shifts introduced at high frequencies by the instrumentation were corrected by feeding a test signal from a small ohmic resistor (in series with

the large resistor in the a.c. circuit) into the analyser and adjusting the phase shift of the reference signal. Complex impedances were determined over the range 10 to 30 000 Hz. Direct current resistances for Cell (b) were obtained from the voltage differences between the electrodes with and without current ($I = 1$ A):

$$R_{dc} = \frac{E(I) - E(0)}{I}. \qquad (1)$$

Charge and discharge resistances (R_c and R_d, respectively) were measured individually by reversing the current appropriately. In addition, sodium was electrolysed into the tube, thus enabling the resistances to be measured for various levels of amalgamation.

The behaviour of the NaNO$_3$/β''-alumina interface [Cell (c)] was investigated by using single current pulses. Amplitudes varied from 0.05 to 0.8 A with a pulse length of 50 ms. The voltage between the two platinum reference electrodes was recorded on the digital oscilloscope.

3. Experimental results

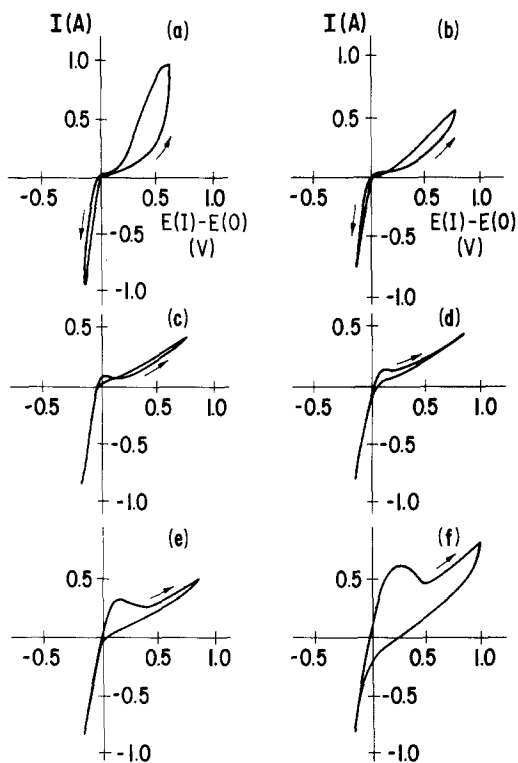Voltammetric current–potential curves for Cell (a) are shown at different sweep rates in Figs. 2a–e.

Fig. 2. Voltammetric current–potential curves for Cell (a). (a) 0.001, (b) 0.01, (c) 0.1, (d) 1, (e) 10, (f) 100 V s^{-1}.

The curve shape appears to have a strong sweep-rate dependence. When similar scans were applied to a β''-alumina with symmetric behaviour, a straight line was observed at all sweep rates (10^{-3} to 10^2 V s^{-1} [3]. In this case a purely ohmic response was attained.

A transition from the blocking interface, Hg/β''-alumina, to the nonblocking interface, Hg(Na)/β''-alumina occurs in Cell (b) when sodium is deposited into the mercury. The transition is indicated by the different complex impedance plots in Figs. 3a and b. The data are presented for a series circuit. In Fig. 3a the measurements were taken prior to any sodium electrolysis and voltage responses were unstable at frequencies below 300 Hz. However, after very brief sodium deposition (36 C), a more stable characteristic was displayed (Fig. 3b). Two semicircles seem to appear in the complex plane plot. With increasing sodium deposition, the phase angle decreased for all frequencies. This is illustrated in Fig. 4 where the ohmic component is plotted at 10 kHz and 10 Hz for various amounts of sodium electrolysis. R_d and R_c are also shown.

The response of Cell (c) to a single 50 ms square pulse consists of a sudden voltage increase, a gradual change in voltage during the pulse itself and a sudden voltage drop at the end of the pulse. The instantaneous voltage change at the inception and completion of the current pulse was measured directly from the digital oscilloscope. This enables a point by point current–voltage curve to be derived, as shown in Fig. 5.

4. Discussion

The various cell configurations enable three different liquid electrode/β''-alumina interfaces to be evaluated. In the classification used by Raleigh [6] these are: parent metal electrode/β''-alumina [Cell (a)], and parent metal solid solution/β''-alumina [Cell (b) with Na–Hg]. The NaNO$_3$/β''-alumina interface is common to all three cases
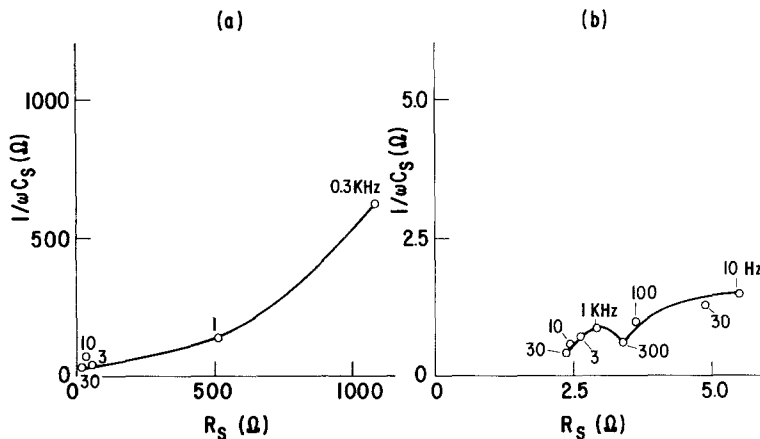

Fig. 3. Plots of the capacitive component versus the ohmic component of the a.c. impedance at different frequencies for Cell (b). (a) Before the start of Na deposition; (b) after 36 C of sodium deposition.
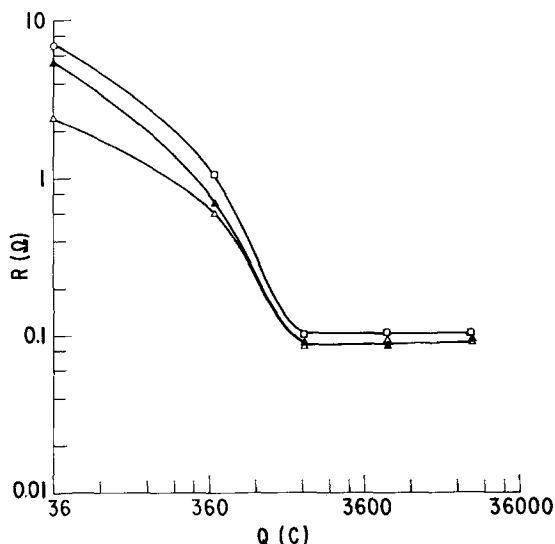
Fig. 4. D.c. resistance and ohmic component of a.c. impedance as a function of sodium deposition for Cell (b). o, D.c., charge; △, a.c., 10 kHz; □, d.c., discharge; ▲, a.c. 10 Hz.

Fig. 5. Plot of the amplitude of the 50 ms current pulse versus the instantaneous voltage change for Cell (c).

and is characterized in Cell (c). Establishing the ohmic behaviour of this interface is an essential step and is considered below.

4.1. The NaNO₃/β″-alumina interface

Despite the scatter in Fig. 5, it is clear that this interface displays an ohmic response for all current densities. The slope of the straight line yields an effective resistance of $0.069\,\Omega$. This compares favourably with the value $0.060\,\Omega$ computed from four-probe bulk conductivities. Since the data in Fig. 5 contain a small contribution from IR drops inside the nitrate on both sides of the tube, it is concluded that there is little polarization at the $NaNO_3$/β″-alumina interface (a polarization effect would imply that the transport of sodium ions between the solid electrolyte and the molten salt is hindered). The ohmic behaviour observed with Cell (c) was limited to single, short pulses. When longer pulses or periodic pulses were applied, the voltage–time traces changed their shape with time. There was some evidence that this was due to the interior platinum electrode and totally independent of the solid electrolyte. A thorough study, however, was not performed. The ohmic nature of the $NaNO_3$/β″-alumina interface and the virtual absence of any significant contact resistance allows
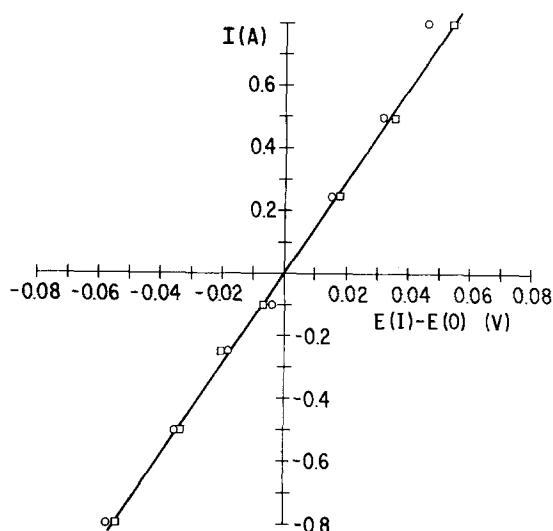
the properties of the other liquid electrode/β″-alumina interfaces to be more readily discerned.

4.2. The Na/β″-alumina interface

Previous work has indicated that the presence of any polarization at this interface seems to be related to the ceramic composition and its propensity to form a Na_2O interfacial film when in contact with molten sodium [1]. The asymmetric behaviour of the β″-alumina tube used in this investigation is illustrated in Figs. 2a–f. The $|I|$ values for a given $|E(I)-E(0)|$ are larger during sodium deposition than during sodium dissolution. In addition the shape of the current–potential curve changes strongly with sweep rate. The large hysteresis observed during sodium dissolution for sweep rates below $0.1\,V\,s^{-1}$ reflects the time dependence of R_d [3]. The higher current during the backward sweep is analogous to the steady-state and long-pulse results [3]. At faster sweep rates the hysteresis disappears because the low resistance state is a relatively slow process. In contrast, the resistance during sodium deposition is virtually independent of sweep rate. A small hysteresis is observed below $0.01\,V\,s^{-1}$.

As the hysteresis becomes smaller with increasing sweep rate, another effect begins to occur. A wave, which is barely noticeable at $0.01\,V\,s^{-1}$

during the upward scan of sodium dissolution, increases in height. The wave is characteristic of an electrochemical reaction, and the results in Fig. 2d–f suggest that the wave is due to subtle changes in the defect structure of an Na_2O film. The film is present at open circuit and is modified during the sweeps. The asymmetric response persists. The resistance during the backward scan (after the wave is completed) is considerably larger than the resistance during sodium deposition for even the fastest sweep rates ($500 \, V \, s^{-1}$). The ohmic behaviour of the $NaNO_3/\beta''$-alumina interface confirms that the voltammetric waves and the asymmetry originate from the Na/β''-alumina interface. With other β''-alumina compositions, symmetric behaviour and other types of asymmetry (time independent) may be observed [3].

4.3. The Hg(Na)/β''-alumina interface

The Hg/β''-alumina interface resembles the ideal polarizable electrode of aqueous electrochemistry. Its properties, however, were not evaluated. Instead the transition between a blocking and a nonblocking electrode was studied by electrolysing Na into the Hg and periodically measuring a.c. and d.c. resistances. The difference in the impedance plots of Fig. 3 has already been attributed to this transition. A second effect, however, must be considered. It is likely that the wetting of the inner surface of the tube by mercury is initially rather poor. Thus the data in Fig. 3a are characteristic of a blocking electrode with poor wetting ability. Deposition of sodium not only alters the character of the electrode, but also improves the wetting between liquid metal and the solid electrolyte. A separation of these two effects is not feasible on the basis of the present results and consequently prevents an unambiguous interpretation of the complex impedance plot.

Fig. 4 shows a decrease in resistance is sodium is deposited into the mercury. Initially there is a relatively wide spread between d.c. and a.c. values. After 1080 C the spread becomes rather small. The a.c. impedance is nearly ohmic, and the values of the ohmic component at 10 kHz and 10 Hz do not differ very much. R_{dc} ($0.10 \, \Omega$) is comparable to the average ohmic component of the a.c. impedance ($0.088 \, \Omega$), but both values are somewhat larger than the computed bulk resistance of the β''-alumina tube ($0.06 \, \Omega$). There is a small contribution from either the Hg(Na)/β''-alumina interface or the $NaNO_3/\beta''$-alumina interface. It is suggested that the contribution is mainly from the Hg(Na) interface since the short-time behaviour of the $NaNO_3$ interface (see Fig. 5) does not allow a contribution of $0.03 \, \Omega$.

Another interesting result present in Fig. 4 is that $R_d = R_c$ after 1080 C (at 360 C there was insufficient sodium during discharge to maintain a current without concentration gradients in the amalgam). That is, there is no asymmetry at the Hg(Na)/β''-alumina interface. In contrast, there is marked asymmetry at the Na/β''-alumina interface under equivalent conditions of sodium electrolysis. This suggests that the oxidation properties of the amalgam either prevent a Na_2O interfacial film from developing or greatly inhibit its formation.

References

[1]   M. W. Breiter, B. Dunn and R. W. Powers, *Electrochim. Acta* **25** (1980) 613.
[2]   D. S. Demott, *J. Electrochem. Soc.* **127** (1980) 2312.
[3]   M. W. Breiter and B. Dunn, *Electrochim. Acta* (in press).
[4]   'Development of Sodium–Sulphur Batteries for Utility Application', *EPRI Report EM-683, Project 128-4, May* (1978).
[5]   B. Dunn, *J. Amer. Ceram. Soc.* **64** (1981) 125.
[6]   D. O. Raleigh, *J. Electroanal. Chem.* **6** (1973) 87.